ORIGINAL RESEARCH • EVIDENCE-BASED PRACTICE

Radiology

CT/MRI and CEUS LI-RADS Major Features Association with Hepatocellular Carcinoma: Individual Patient Data Meta-Analysis

Christian B. van der Pol, MD • Matthew D. F. McInnes, MD, PhD • Jean-Paul Salameh, MSc • Brooke Levis, PhD • Victoria Chernyak, MD, MS • Claude B. Sirlin, MD • Mustafa R. Bashir, MD • Brian C. Allen, MD • Lauren M. B. Burke, MD • Jin-Young Choi, MD, PhD • Sang Hyun Choi, MD • Alejandro Forner, MD • Tyler J. Fraum, MD • Alice Giamperoli, MD • Hanyu Jiang, MD • Ijin Joo, MD • Zhen Kang, MD • Andrea S. Kierans, MD • Hyo-Jin Kang, MD • Gaurav Khatri, MD • Jung Hoon Kim, MD • Myeong-Jin Kim, MD, PhD • So Yeon Kim, MD • Yeun-Yoon Kim, MD • Heejin Kwon, MD • Jeong Min Lee, MD • Sara C. Lewis, MD • Katrina A. McGinty, MD • Lorenzo Mulazzani, MD • Mi-Suk Park, MD • Fabio Piscaglia, MD • Joanna Podgórska, MD • Caecilia S. Reiner, MD • Maxime Ronot, MD, PhD • Grzegorz Rosiak, MD, PhD • Bin Song, MD • Ji Soo Song, MD • An Tang, MD • Eleonora Terzi, MD • Jin Wang, MD • Wei Wang, MD • Stephanie R. Wilson, MD • Takeshi Yokoo, MD, PhD

From the Dept of Diagnostic Imaging, Juravinski Hosp and Cancer Centre, Hamilton Health Sciences, McMaster Univ, Hamilton, Canada (C.B.v.d.P.); Dept of Radiology and Epidemiology, Univ of Ottawa, Ottawa, Canada (M.D.F.M.); Ottawa Hosp Research Inst Clinical Epidemiology Program, Dept of Medical Imaging, the Ottawa Hosp-Civic Campus, 1053 Carling Ave, Room c-159, Ottawa, ON, Canada K1E 4Y9 (M.D.F.M.); Faculty of Health Sciences, Queen's Univ, Kingston, Canada (J.P.S.); Clinical Epidemiology Program, Ottawa Hosp Research Inst, Ottawa, Canada (J.P.S.); Centre for Prognosis Research, School of Medicine, Keele Univ, Staffordshire, UK (B.L.); Dept of Radiology, Montefiore Medical Ctr, Bronx, NY (V.C.); Liver Imaging Group, Dept of Radiology, Univ of California San Diego, San Diego, Calif (C.B.S.); Depts of Radiology (M.R.B., B.C.A.) and Medicine (M.R.B.) and Ctr for Advanced Magnetic Resonance Development (M.R.B.), Duke Univ Medical Ctr, Durham, NC; Dept of Radiology, Univ of North Carolina, Chapel Hill, NC (M.R.B., L.M.B.B., K.A.M.); Dept of Radiology, Research Inst of Radiological Science, Yonsei Univ College of Medicine, Seoul, Korea (J.Y.C., M.J.K., Y.Y.K., M.S.P.); Asan Medical Ctr, Univ of Ulsan College of Medicine, Seoul, Korea (S.H.C.); BCLC Group, Liver Unit, Hosp Clínic of Barcelona, Barcelona, Spain (A.F.); IDIBAPS, CIBERehd, Univ of Barcelona, Barcelona, Spain (A.F.); Mallinckrodt Inst of Radiology, Washington Univ School of Medicine, St Louis, Mo (T.J.F.); Div of Internal Medicine, Hepatobiliary and Immunoallergic Diseases (A.G., F.P., E.T.), and Emergency Dept, Medicina d'Urgenza e Pronto Soccorso (L.M.), IRCCS Azienda Ospedaliero-Universitaria di Bologna, Bologna, Italy; Dept of Radiology, West China Hosp, Sichuan Univ, Chengdu, China (H.J.); Dept of Radiology (I.J., H.J.K., J.H.K., J.M.L.) and Inst of Radiation Medicine (J.H.K., J.M.L.), Seoul National Univ Hosp, Seoul, Korea; Dept of Radiology, Seoul National Univ College of Medicine, Seoul, Korea (I.J., J.H.K., J.M.L.); Dept of Radiology, Tongji Hosp, Tongji Medical College, Wuhan, China (Z.K.); Huazhong Univ of Science and Technology, Wuhan, China (Z.K.); Dept of Radiology, Weill Cornell Medical Ctr, New York, NY (A.S.K.); Dept of Radiology (G.K., T.Y.) and Advanced Imaging Research Ctr (T.Y.), Univ of Texas Southwestern Medical Ctr, Dallas, Tex; Dept of Radiology and Research Inst of Radiology, Univ of Ulsan College of Medicine, Asan Medical Ctr, Seoul, Korea (S.Y.K.); Dept of Radiology, Dong-A Univ Hosp, Dong-A Univ College of Medicine, Busan, Korea (H.K.); Dept of Radiology, Icahn School of Medicine at Mount Sinai, New York, NY (S.C.L.); 2nd Radiology Dept, Warsaw Medical Univ, Warsaw, Poland (J.P., G.R.); Inst of Diagnostic and Interventional Radiology, Univ Hosp Zurich, Zurich, Switzerland (C.S.R.); Dept of Radiology, Beaujon Hosp, APHP.Nord, Clichy, France (M.R.); Université de Paris, Paris, France (M.R.); Dept of Radiology, West China Hosp, Sichuan Univ, Chengdu, China (B.S.); Dept of Radiology, Jeonbuk National Univ Medical School and Hosp, Jeonju, Korea (J.S.S.); Dept of Radiology, Centre Hospitalier de l'Université de Montréal, Montréal, Canada (A.T.); Dept of Radiology, the Third Affiliated Hosp, Sun Yat-sen Univ, Guangzhou, China (J.W.); Dept of Medical Ultrasonics, Inst of Diagnostic and Interventional Ultrasound, the First Affiliated Hosp of Sun Yat-Sen Univ, Guangzhou, China (W.W.); Depts of Radiology and Medicine, Div of Gastroenterology, Univ of Calgary, Calgary, Canada (S.R.W.); and Foothills Medical Centre, Calgary, Canada (S.R.W.). Received May 17, 2021; revision requested Jul 15; revision received Sept 1; accepted Sept 14. **Address correspondence to** M.D.F.M. (e-mail: *mmcinnes@toh.ca*).

Supported by a grant from the Joan Sealy Trust for Cancer Research, a Fonds de Recherche du Québec–Santé postdoctoral training fellowship (B.L.), the Sichuan Province Science and Technology Support Program (2021YFS0141) (H.J.), and the Fonds de Recherche du Québec–Santé and Fondation de l'Association des Radiologistes du Québec (34939, 298509) (A.T.).

Conflicts of interest are listed at the end of this article.

Radiology 2022; 302:326–335 • https://doi.org/10.1148/radiol.2021211244 • Content codes: GI CT MR

Background: The Liver Imaging Reporting and Data System (LI-RADS) assigns a risk category for hepatocellular carcinoma (HCC) to imaging observations. Establishing the contributions of major features can inform the diagnostic algorithm.

Purpose: To perform a systematic review and individual patient data meta-analysis to establish the probability of HCC for each LI-RADS major feature using CT/MRI and contrast-enhanced US (CEUS) LI-RADS in patients at high risk for HCC.

Materials and Methods: Multiple databases (MEDLINE, Embase, Cochrane Central Register of Controlled Trials, and Scopus) were searched for studies from January 2014 to September 2019 that evaluated the accuracy of CT, MRI, and CEUS for HCC detection using LI-RADS (CT/MRI LI-RADS, versions 2014, 2017, and 2018; CEUS LI-RADS, versions 2016 and 2017). Data were centralized. Clustering was addressed at the study and patient levels using mixed models. Adjusted odds ratios (ORs) with 95% CIs were determined for each major feature using multivariable stepwise logistic regression. Risk of bias was assessed using Quality Assessment of Diagnostic Accuracy Studies 2 (QUADAS-2) (PROSPERO protocol: CRD42020164486).

Results: A total of 32 studies were included, with 1170 CT observations, 3341 MRI observations, and 853 CEUS observations. At multivariable analysis of CT/MRI LI-RADS, all major features were associated with HCC, except threshold growth (OR, 1.6; 95% CI: 0.7, 3.6; $P = .07$). Nonperipheral washout (OR, 13.2; 95% CI: 9.0, 19.2; $P = .01$) and nonrim arterial phase hyperenhancement (APHE) (OR, 10.3; 95% CI: 6.7, 15.6; $P = .01$) had stronger associations with HCC than enhancing capsule (OR, 2.4; 95% CI: 1.7, 3.5; $P = .03$). On CEUS images, APHE (OR, 7.3; 95% CI: 4.6, 11.5; $P = .01$), late and mild washout (OR, 4.1; 95% CI: 2.6, 6.6; $P = .01$), and size of at least 20 mm (OR, 1.6; 95% CI: 1.04, 2.5; $P = .04$) were associated with HCC. Twenty-five studies (78%) had high risk of bias due to reporting ambiguity or study design flaws.

Conclusion: Most Liver Imaging Reporting and Data System major features had different independent associations with hepatocellular carcinoma; for CT/MRI, arterial phase hyperenhancement and washout had the strongest associations, whereas threshold growth had no association.

Online supplemental material is available for this article.

Abbreviations

APHE = arterial phase hyperenhancement, CEUS = contrast-enhanced US, HCC = hepatocellular carcinoma, IPD = individual patient data, LI-RADS = Liver Imaging Reporting and Data System, OR = odds ratio, QUADAS = Quality Assessment of Diagnostic Accuracy Studies

Summary

Most CT/MRI and CEUS LI-RADS major features had independent associations with hepatocellular carcinoma; arterial phase hyperenhancement and washout had the strongest associations whereas, for CT/MRI, threshold growth had no association.

Key Results

- In this meta-analysis of 32 studies with 1170 CT observations, 3341 MRI observations, and 853 contrast-enhanced US (CEUS) observations, all CT/MRI Liver Imaging Reporting and Data Systems (LI-RADS) major features except threshold growth (odds ratio [OR], 1.6; $P = .07$) were independently associated with hepatocellular carcinoma (HCC).
- On CEUS images, arterial phase enhancement (OR, 7.3; $P = .01$), late and mild washout (OR, 4.1; $P = .01$), and size of at least 20 mm (OR, 1.6; $P = .04$) were associated with HCC.

The Liver Imaging Reporting and Data System (LI-RADS) is used to assign a risk category of hepatocellular carcinoma (HCC) to liver observations at imaging in patients at high risk for HCC. LI-RADS algorithms have been developed for screening (US), diagnosis (CT/MRI and contrast-enhanced US [CEUS]), and after local-regional treatment assessment. The LI-RADS framework aims to standardize reporting and data collection of imaging for HCC to enhance communication, reduce interobserver variability, and facilitate quality assurance and research (1). LI-RADS is regularly updated to achieve these aims as new evidence emerges.

The CT/MRI diagnostic algorithm uses a combination of major features (size, nonrim arterial phase hyperenhancement [APHE], nonperipheral washout, enhancing capsule, and threshold growth) to assign categories. Similarly, CEUS uses a combination of major features (size, nonrim APHE, and late and mild washout) to assign categories. In both diagnostic algorithms, each category reflects a relative probability of benignity, malignancy in general, or HCC. Recent systematic reviews found that the percentage of HCC (equivalent to positive predictive value) differed for each CT/MRI LI-RADS category and increased as LI-RADS category increased (2–4). Limitations of these reviews include the lack of individual patient data (IPD) to determine the independent impact of each of the major imaging features on the final diagnosis of HCC. Therefore, it remains unclear if some major features increase the likelihood of HCC more than others, whether features should be assigned different weights, or if some major features are unnecessary and could be eliminated. Understanding the relative contributions of imaging features to system performance is important for continued development and improvement of LI-RADS, which could be achieved using IPD meta-analysis (5).

Given the many LI-RADS imaging features, it is challenging for a single study to achieve sufficient statistical power to analyze the impact of each imaging feature. An IPD meta-analysis would improve understanding of which imaging features drive LI-RADS performance. The IPD meta-analyses use large and detailed data sets at the patient level to perform more complex subgroup analysis than can be achieved in any single study or by using meta-analysis of aggregate study-level data (6). These involve collecting and pooling de-identified primary patient data from authors of prior publications (7). The purpose of this systematic review and IPD meta-analysis was to establish the likelihood of HCC for each LI-RADS major feature using CT/MRI LI-RADS and CEUS LI-RADS in patients at high risk for HCC.

Materials and Methods

The study protocol was approved by the Ottawa Hospital Research Ethics Board, is Health Insurance Portability and Accountability Act compliant, and was registered on PROSPERO (CRD42020164486). Methodologic guidance was per best practice in diagnostic test accuracy systematic reviews (8,9). Reporting is in accordance with the Preferred Reporting Items for a Systematic Review and Meta-analysis of Diagnostic Test Accuracy Studies and Individual Patient Data (10–14).

Eligibility Criteria

All CT, MRI, and CEUS studies reporting the percentage of HCC and overall malignancy for LI-RADS categories 1–5, tumor in vein, and malignancy in patients at high risk of HCC (hepatic cirrhosis, chronic hepatitis B viral infection, current or prior HCC) were eligible for inclusion. The CT, MRI, and CEUS techniques were evaluated for each study to determine concordance with the LI-RADS technical imaging guidelines (15). All liver observations were required to have been categorized using CT/MRI LI-RADS version 2014, 2017, or 2018 or CEUS LI-RADS version 2016 or 2017 (16–20). A preferred reference standard was established to assess bias risk (Appendix E1 [online]).

Database Search and Study Selection

With the assistance of an experienced hospital librarian, we performed a search of the MEDLINE, Embase, Cochrane Central Register of Controlled Trials, and Scopus databases for studies from January 2014 to September 2019 that evaluated the diagnostic accuracy of CT, MRI, or CEUS for HCC using LI-RADS (Appendix E2 [online]). The corresponding authors of each study identified for inclusion were contacted (Appendix E3 [online]).

Data Collection Process and Definitions for Data Extraction

Authors who did not respond to the invitation to collaborate were sent follow-up emails in an effort to maximize data set size. All authors agreeing to participate were sent a formal confidentiality agreement explaining that data would be stored securely and only accessed by authorized coinvestigators with a copy of the data contribution form, data extraction sheet, data dictionary, and a list of frequently asked questions (Appendixes E4–E7 [online]). The request for de-identified data included instructions to transfer data to an encrypted directory. On the basis of institutional policies, when necessary, data sharing agreements were obtained. Efforts were made to keep all collaborators in-

volved and informed of progress. IPD were not distributed elsewhere.

Risk of Bias and Applicability

A previously customized Quality Assessment of Diagnostic Accuracy Studies 2 (QUADAS-2) tool for application to LI-RADS in a prior study-level systematic review was modified to assess risk of bias for each data set (Appendix E8 [online]) (2). QUADAS-2 divides sources of bias into four categories, including patient selection, index test, reference standard, and flow and timing (21,22). Incomplete reporting of major features was flagged using QUADAS-2 under the flow and timing domain. Risk of bias and applicability assessment were performed in duplicate and independently by two authors (C.B.v.d.P., J.P.S.; each with experience conducting risk of bias assessment for diagnostic test accuracy studies), and differences were resolved by discussion with a third author (M.D.F.M.). A pilot of one study with subsequent discussion was performed by these three authors to improve subsequent interobserver agreement.

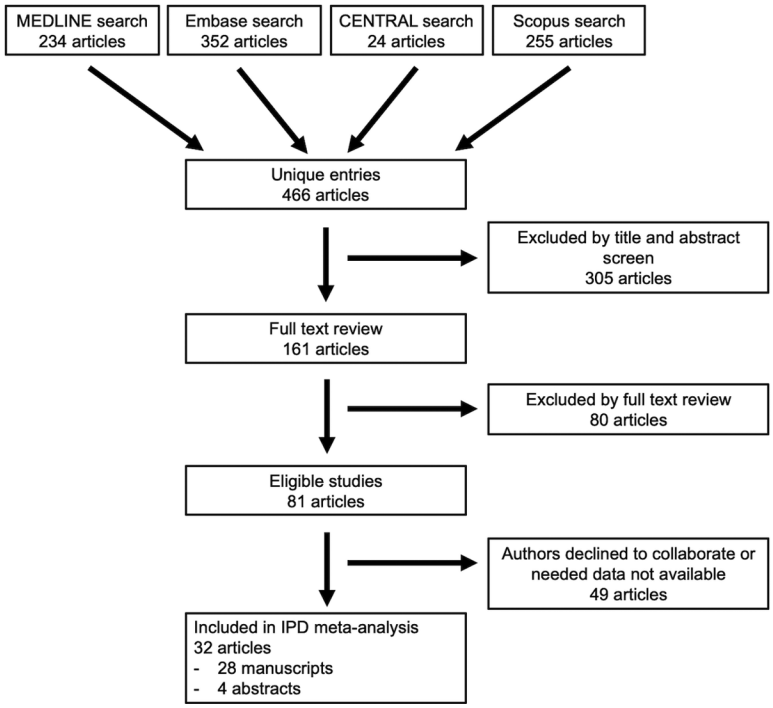

Figure 1: Flow diagram shows search results, study review, and study inclusion. CENTRAL = Cochrane Central Register of Controlled Trials, IPD = individual patient data.

Diagnostic Accuracy Measures

The main model estimates of interest were odds ratios (ORs) to determine the association of each LI-RADS major feature with a diagnosis of HCC, both independently and in combination.

Synthesis of Results

All data were pooled into a master data set, with each observation assigned a unique identifier. IPD received from primary study investigators were compared against the published reports for each study. When data were unclear or inconsistent, primary study investigators were contacted to resolve the differences (nine studies). When multiple readers were present, the data from one reader was chosen at random (six studies). One study included observations made with an extracellular contrast agent and the same observations made again with a hepatobiliary-specific contrast agent. Examinations using the contrast agent less represented in our cohort (gadoxetic acid) were included to improve representation of that agent.

Statistical Analysis

We used a one-step IPD meta-analysis approach to pool the IPD across studies and model them simultaneously to compute OR for the association of each LI-RADS major feature with HCC (Appendix E9 [online]). Liver observation clustering was addressed at the study and patient levels through random intercepts. The ORs for all the variables are presented with 95% CIs. Collinearity between variables was assessed by calculating the variance inflation factor, the tolerance statistic, and eigenvalues. The strength of the association of the variables with the outcome of interest was determined based on the statistical significance and the magnitude of the ORs derived in the multivariable model. A sensitivity analysis was performed by limiting the same analyses to studies at overall low risk of bias. Forest plots show individual study results. τ^2 was used to quantify heterogeneity, and funnel plots were generated to demonstrate publication bias. The level of significance was set at $P < .05$. All analyses were performed by study authors (J.P.S., B.L.) using the glmer function in the Lme4 package in R (R Core Team, version 4.0.0; R Foundation for Statistical Computing) (23).

Results

Study Selection and Characteristics

A total of 865 studies were identified during the initial search, with 466 remaining once duplicates were removed. On title and abstract review, 161 studies were identified for possible inclusion (Fig 1). After full-text review, authors of 81 studies were invited to collaborate, 47 of whom agreed and 37 of whom provided data (Appendix E10 [online] lists studies whose authors did not respond). Studies were then excluded at this stage for the following reasons: incomplete and redundant data with other studies (24,25), multisite data not readily available (26), only patient-level and not observation-level data were available (27), and data formatting issues precluding extraction of relevant parameters (28). The final cohort included 32 studies, including 28 articles and four published conference abstracts (Table 1) (29–60).

Risk of Bias and Applicability

Of the 32 studies, seven were considered at low risk of bias, and 23 had low concern regarding applicability (Fig 2). Study flow

Table 1: Characteristics of Included Studies

				Imaging Technique				Observation Data											
Ref No.	Country	Design	Prevailing Risk Factor*	Modality	Contrast Agent	LI-RADS Version	No. of Readers	No. of Liver Observations/ No. of Patients	No. of HCCs	No. Overall Malignancy	No. Benign	No. LR-1	No. LR-2	No. LR-3	No. LR-4	No. LR-5	No. LR-TIV/5 V	No. LR-M	Ref Standard
29	Can	RC	Cirrhosis > > HBV	CT	ECA	2017	2	91/39	72 (79)	76	15	1	5	9	25	38	10	3	P and CCRS
30	USA	RCCon	Cirrhosis > > HBV	MRI	ECA, HPB	2014	3	47/36	42	45	2	0	0	10.3	11	25.7	0	0	P and CCRS
31	Kor	RC	HBV > > cirrhosis	MRI	HPB	2014	2	225/225	218 (97)	225	0	0	0	1	43	170	0	11	P
32	Can	RC	Cirrhosis > > HBV	MRI	ECA	2014	2	275/102	113 (41)	123	152	38	52	57	53	58	2	15	P and CCRS
33	Chi	RC	HBV > cirrhosis	MRI	ECA, HPB	2018	2	149/149	149 (100)	149	0	0	0	0	0	149	0	0	P
34	Chi	RCCon	HBV with cirrhosis	CEUS	Blood pool	2017	2	176/176	88 (50)	176	0	0	0	1	6	49	0	120	P
35	Kor	RC	HBV > cirrhosis	MRI	HPB	2018	NR	372/258	273 (73)	291	81	0	0	18	154	180	4	16	P and CCRS
36	Spain	RC	Cirrhosis	MRI	ECA	2018	NR	262/262	197 (75)	204	58	15	26	74	12	127	0	8	P and CCRS
37	USA	RC	Cirrhosis > > HBV	CT, MRI	CT: ECA MRI: ECA	2014	2	CT: 7/7 MRI: 213/213	CT: 4 (57) MRI: 132 (62)	CT: 7 MRI: 171	CT: 0 MRI: 42	CT: 0 MRI: 4	CT: 0 MRI: 10.5	CT: 0 MRI: 10.5	CT: 0.5 MRI: 34	CT: 2 MRI: 93.5	CT: 1.5 MRI: 11	CT: 3 MRI: 49.5	P
38	Can	PC	Cirrhosis > > HBV	CEUS, MRI	CEUS: Blood pool MRI: ECA, HPB	CEUS: 2017 MRI: 2018	2	CEUS: 39/35 MRI: 38/34	CEUS: 11 (28) MRI: 11 (29)	CE US: 12 MRI: 12	CE US: 27 MRI: 26	CE US: 22 MRI: NR	CE US: 1 MRI: NR	CE US: 4 MRI: NR	CE US: 1 MRI: NR	CE US: 10 MRI: NR	CE US: 0 MRI: NR	CE US: 1 MRI: NR	P and CCRS
39	Kor	RCCon	HBV > > cirrhosis	MRI	HPB	2017	2	140/140	70 (50)	140	0	0	0	0	21	67	2	50	P
40	Chi	PC	HBV > > cirrhosis	MRI	HPB	2018	2	272/272	215 (79)	254	18	1	3	4	28	151	57	28	P and CCRS
41	Kor	RC	HBV > > cirrhosis	CT, MRI	CT: ECA MRI: HPB	2014	2	216/158	216 (100)	216	0	CT: 0 MRI: 0	CT: 0 MRI: 0	CT: 23.5 MRI: 5.5	CT: 55.5 MRI: 74	CT: 129 MRI: 128	CT: 6 MRI: 6	CT: 2 MRI: 2.5	P
42	Kor	PC	HBV > cirrhosis	CEUS, CT, MRI	CEUS: blood pool CT: ECA MRI: HPB	2017	2	CEUS: 43/43 CT: 35/35 MRI: 8/8	CEUS: 20 (47) CT: 16 (46) MRI: 4 (50)	CE US: 21 CT: 17 MRI: 4	CE US: 22 CT: 18 MRI: 4	0	0	CE US: 16 CT: NR MRI: NR	CE US: 16 CT: NR MRI: NR	CE US: 10 CT: 0 MRI: 0	0	CE US: 1 CT: 0 MRI: 0	P and CCRS
43	Chi	RC	Cirrhosis, no other details	MRI	ECA	2014	2	19/19	15 (79)	17	2	0	0	4	2	11	1	1	P and CCRS
44	USA	RC	Cirrhosis > HBV	MRI	ECA, HPB	2017	3	144/98	82 (57)	90	54	5	8	45	25	41	10	10	P and CCRS
45	Kor	RC	HBV > > cirrhosis	MRI	HPB	2018	2	203/160	186 (92)	197	6	NR	NR	NR	NR	NR	NR	NR	P
46	Kor	RC	HBV > > cirrhosis	MRI	HPB	2014	1	202/109	129 (64)	135	67	11	27	42	29	75	5	13	P and CCRS
47	Kor	RCCon	Cirrhosis, most had HBV	MRI	HPB	2018	2	220/220	165 (75)	220	0	0	0	5	10	70	0	135	P

Table 1 (*continues*)

Table 1 (*continued*): Characteristics of Included Studies

				Imaging Technique				Observation Data											
Ref No.	Country	Design	Prevailing Risk Factor*	Modality	Contrast Agent	LI-RADS Version	No. of Readers	No. of Liver Observations/ No. of Patients	No. of HCCs	No. Overall Malignancy	No. Benign	No. LR-1	No. LR-2	No. LR-3	No. LR-4	No. LR-5	No. LR-TIV/5 V	No. LR-M	Ref Standard
48	Kor	RCCon	HBV > cirrhosis	MRI	HPB	2017	2	99/99	66 (67)	99	0	NR	NR	NR	NR	NR	NR	65	P
49	USA	RC	HBV ~ cirrhosis	MRI	ECA, HPB	2017	2	65/63	36 (55)	65	0	0	0	0	0.5	26	5.5	33	P
50	Kor	RC	Cirrhosis >> HBV	MRI	HPB	2018	2	65/65	23 (35)	58	7	0	0	0	0	0	0	65	P
51	Can	RC	Cirrhosis >> HBV	CEUS	Blood pool	2016	3	196/184	139 (71)	157	39	10	1	24	8	116	8	29	P and CCRS
52	Italy	PC	Cirrhosis >> HBV	CEUS	Blood pool	2017	NR	54/34	33 (61)	34	20	6	3	4	7	25	3	1	P and CCRS
53	France	PC	Cirrhosis >> HBV	CT, MRI	ECA	2014	1	CT: 528/292 MRI: 562/300	CT: 323 (61) MRI: 328 (58)	NR	NR	NR	NR	NR	CT: 116 MRI: 132	CT: 98 MRI: 95	CT: 242 MRI: 264	CT: 11 MRI: 6	0	P and CCRS
54	Poland	RC	Cirrhosis >> HBV	MRI	HPB	2017	2	69/18	50 (72)	50	19	0	0	18	13	38	0	0	P
55	Kor	RC	HBV ~ cirrhosis	CT	ECA	2014	2	R1: 67/50 R2: 102/65	R1: 42 (63) R2: 54 (53)	NR	NR	R1: 11 R2: 16	R1: 1 R2: 18	R1: 11 R2: 14	R1: 16 R2: 21	R1: 28 R2: 31	NR	R1: 0 R2: 2	P
56	Kor	RC	HBV ~ cirrhosis	MRI	ECA, HPB	2014	2	77/52	77 (100)	77	0	0	0	ECA: 1 HPB: 1	ECA: 25 HPB: 39	ECA: 51 HPB: 37	0	0	P and CCRS
57	Switz-erland	RC	Cirrhosis >> HBV	MRI	ECA	2018	4	71/51	28 (39)	28	43	18	11	15	6	21	0	0	P and CCRS
58	Italy	RC	Cirrhosis >> HBV	CEUS	Blood pool	2017	NR	333/NR	278 (83)	289	44	0	0	74	97	144	0	18	P and CCRS
59	Can	RC	Cirrhosis >> HBV	MRI	ECA, HPB	2018	2	222/81	72 (32)	72	150	23	33	68	42	56	0	0	P and CCRS
60	Chi	RC	HBV >> cirrhosis	MRI	ECA, HPB	2018	2	82/80	82 (100)	82	0	0	0	7	7	68	0	0	P

Note.— Data were averaged if there was more than one reader. Data in parentheses are percentages. Studies were considered case control studies if groups of patients were selected based on final diagnosis and then imaging findings were compared. Gadobenate dimeglumine was documented as a hepatobiliary contrast agent if hepatobiliary phase imaging was used; otherwise, it was considered an extracellular agent. Can = Canada, Chi = China, CCRS = composite reference standard, CEUS = contrast-enhanced US, ECA = extracellular contrast agent, HPB = hepatobiliary contrast agent, Kor = Korea, NR = not recorded, P = pathology, PC = prospective cohort, RC = retrospective cohort, RCCon = retrospective case control, Ref = reference, USA = United States.

* The > symbol indicates the first risk factor was more represented in the cohort than the second risk factor. The ~ symbol indicates both risk factors were represented approximately equally. The >> symbols indicate that the first risk factor was substantially more represented in the cohort than the second risk factor.

and timing was the domain most often at risk for bias, which was usually due to unclear or inappropriate intervals between the index test and the reference standard or verification bias (from tissue sampling of only a subset of observations) (Table E1 [online]). Patient and observation selection were also frequently at risk for bias due to multiple studies with case-control design and studies limited to only patients with malignant lesions. The index test and reference standard domains were at low risk of bias for most studies. Funnel plots are available in Appendix E11 [online].

Synthesis of Results

All observations were classified using either pathology or the composite reference standard (Table 2).

***CT/MRI.*—**A total of 1170 observations obtained with CT in 812 patients from six studies and 3341 observations obtained with MRI in 2639 patients from 17 studies had sufficient data to be incorporated into the model (Table E2 [online]). From these cohorts, 813 observations were obtained with both CT and MRI. All five major features had been assessed for 887 ob-

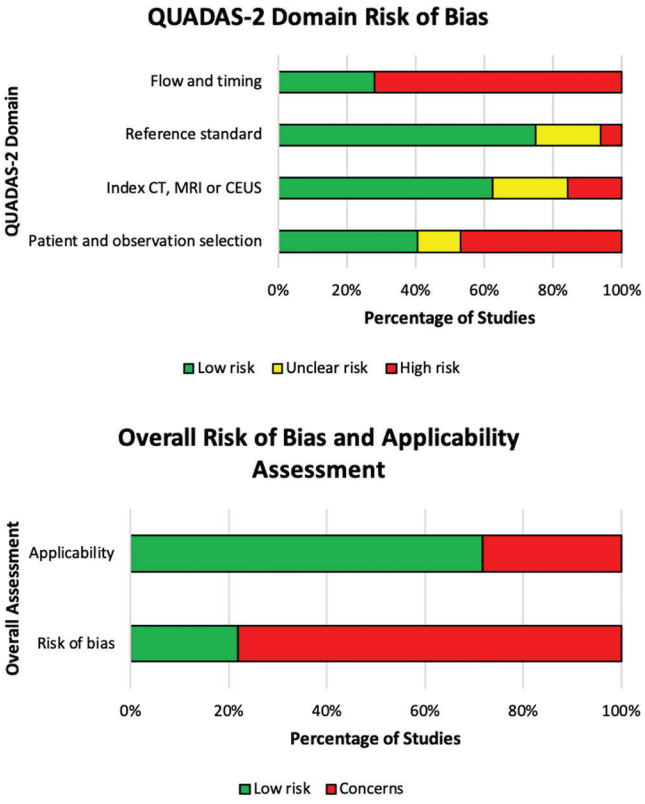

Figure 2: Quality Assessment of Diagnostic Accuracy Studies 2 (QUADAS-2) risk of bias assessment. CEUS = contrast-enhanced US.

Table 2: Observation Diagnosis and Reference Standard

Final Diagnosis	Total No. of Observations	Confirmed with Histology	Confirmed with Composite Reference Standard*
HCC	3582	3011	571
Intrahepatic cholangiocarcinoma	28	28	0
Combined HCC and cholangiocarcinoma	122	122	0
Other specific malignancy	256	256	0
Nonspecific malignancy	3	0	3
Benign	1373	961	412

* Benign if stable for at least 12 months or spontaneous size reduction of at least 30% or disappearance attributable to treatment or resorption of tumoral blood products. Hepatocellular carcinoma (HCC) was diagnosed if LR-5 criteria were fulfilled on another imaging modality study and there was threshold growth, or if LR-5 criteria were fulfilled and recurred after local-regional treatment on CT or MRI scans based on treatment response criteria. Other malignancies required histopathology for confirmation. LR-3, LR-4, and LR-M observations with recurrence on CT or MRI scans after local treatment were considered malignant but not specifically indicative of HCC.

servations, while 3547 observations included assessment of all major features except threshold growth. Threshold growth was the major feature that was reported least often; authors reported that this was due to a lack of prior imaging examinations available for comparison in 75% of studies (21 of 28), rather than a feature of study design.

Results of the univariable analyses are presented in Table E3 (online), which found all five major features to be associated with HCC. Based on the clinical and statistical significance in the univariable analyses, the size variable was investigated as a categorical variable in the multivariable analysis. On multivariable analysis of the cohort including only observations with all five major features assessed (n = 887 observations), all major features were associated with HCC except threshold growth (OR, 1.6; 95% CI: 0.7, 3.6; P = .07) (Fig 3, Table 3). Multivariable analysis was repeated on the subset of observations, with all major features assessed except threshold growth (3547 observations). In this subset, we did not find evidence of association of enhancing capsule with HCC (OR, 1.3; 95% CI: 0.7, 2.5; P = .08). However, when multivariable analysis was performed on the largest cohort including observations with APHE, enhancing capsule, and nonperipheral washout consistently reported (4434 observations), each was associated with HCC. The variance inflation factor, tolerance statistic, and eigenvalues were computed and were within guidelines (61). On sensitivity analysis limited to observations from studies at low risk of bias, these associations persisted (Table E4 [online]).

Using the largest cohort of observations with APHE, enhancing capsule, and nonperipheral washout consistently reported (n = 4434), observation size smaller than 10 mm was associated with decreased odds of HCC diagnosis (OR, 0.1; 95% CI: 0.0, 0.2; P = .01) compared with a size of 10–19 mm. Observation size of at least 20 mm was not associated with HCC compared with a size of 10–19 mm (OR, 1.6; 95% CI: 0.95, 2.7; P = .06).

Of all CT/MRI major features, differences between CT and MRI were found only for observation size. For patients with observations of at least 10 mm on MRI scans, the odds of having HCC were higher than for those imaged with CT, namely 3.6 (95% CI: 1.04, 12.4; P = .04) for 10–19-mm observations and 3.1 (95% CI: 1.9, 5.1; P = .03) for observation 20 mm or larger.

CEUS.—A total of 853 observations were imaged using CEUS in 833 patients from six studies, and assessments of all major features were available. Results of the univariable analysis are presented in Table E5 [online]. On multivariable analysis, the following were associated with HCC: nonrim APHE (OR, 7.3; 95% CI: 4.6, 11.5; P = .01), late and mild washout (OR, 4.1; 95% CI: 2.6, 6.6; P = .01), and size of at least 20 mm (OR, 1.6; 95% CI: 1.04, 2.5; P = .04) compared with 10–19-mm observations (Table 4). Rim or peripheral discontinuous globular enhancement was associated with decreased odds of HCC (OR, 0.3; 95% CI: 0.1, 0.9; P = .02), as was early (<60 seconds) washout (OR, 0.3; 95% CI: 0.1, 0.5; P = .03). Marked washout was not associated with diag-

nosis or nondiagnosis of HCC (OR, 0.7; 95% CI: 0.2, 2.8; P = .10). A sensitivity analysis including only the two CEUS studies at overall low risk of bias was not performed due to model instability.

Forest plots show individual study results (Appendix E12 [online]), and τ^2 was used to quantify heterogeneity (Appendix E13 [online]).

Discussion

This individual patient data (IPD) meta-analysis of 1170 CT, 3341 MRI, and 853 contrast-enhanced US (CEUS) observations found that all Liver Imaging Reporting and Data System (LI-RADS) major features were independently associated with hepatocellular carcinoma (HCC) except for threshold growth. For CT/MRI, nonperipheral washout (odds ratio [OR], 13.2; 95% CI: 9.0, 19.2; P = .01) and nonrim arterial phase hyperenhancement (APHE) (OR, 10.3; 95% CI: 6.7, 15.6; P = .01) had the strongest association with HCC, followed by enhancing capsule (OR, 2.4; 95% CI: 1.7, 3.5; P = .03). Threshold growth was infrequently reported (mostly due to a lack of available prior examinations followed by study design) and was not independently associated with HCC (OR, 1.6; 95% CI: 0.7, 3.6; P = .07). For CEUS, nonrim and nonperipheral discontinuous globular APHE had the strongest association with HCC (OR, 7.3; 95% CI: 4.6, 11.5; P = .01), whereas late and mild washout

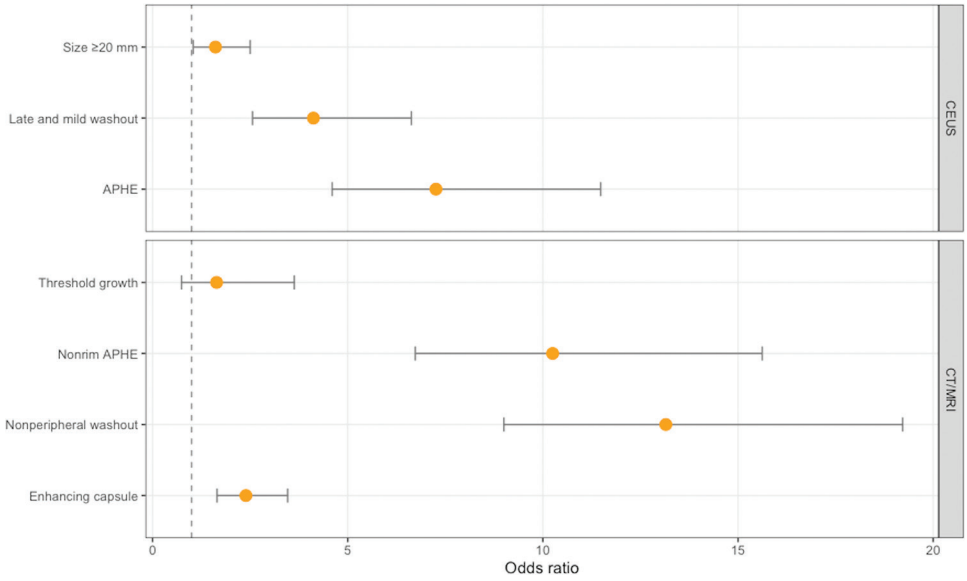

Figure 3: Multivariable analysis odds ratios with 95% CIs (error bars) for the association of each CT/MRI and contrast-enhanced US (CEUS) Liver Imaging Reporting and Data System major feature with a diagnosis of hepatocellular carcinoma. APHE = arterial phase hyperenhancement.

Table 3: CT/MRI Major Features Multivariable Analysis

Major Feature	Observations with All Five Major Features Reported (n = 887)*		Observations with All Major Features Reported Except Threshold Growth (n = 3547)†		Observations with or without Threshold Growth Reported (n = 4434)‡	
	Odds Ratio	P Value	Odds Ratio	P Value	Odds Ratio	P Value
Nonrim APHE	3.6 (1.9, 6.9)	.01	14.5 (7.1, 29.8)	.01	10.3 (6.7, 15.6)	.01
Enhancing capsule	2.3 (1.1, 4.7)	.04	1.3 (0.7, 2.5)	.08	2.4 (1.7, 3.5)	.03
Nonperipheral washout	5.6 (3.0, 10.5)	.02	7.9 (4.4, 14.3)	.01	13.2 (9.0, 19.2)	.01
Size						
<10 mm	0.1 (0.0, 0.3)	.01	0.0 (0.0, 0.4)	.01	0.1 (0.0, 0.2)	.01
10–19 mm	Reference	…	Reference	…	Reference	…
≥20 mm	11.2 (1.9, 65.2)	.03	0.7 (0.3, 1.6)	.07	1.6 (0.95, 2.7)	.06
Threshold growth	1.6 (0.7, 3.6)	.07	…	…	…	…
CT (reference) versus MRI§						
<10 mm	2.4 (0.6, 10.1)	.10	0.9 (0.1, 10.7)	.12	1.2 (0.8, 1.9)	.09
10–19 mm	0.5 (0.2, 1.5)	.06	0.3 (0.2, 0.6)	.03	3.6 (1.04, 12.4)	.04
≥20 mm	0.1 (0.0, 0.5)	.03	6.2 (2.5, 14.9)	.02	3.1 (1.9, 5.1)	.03

Note.—Data in parentheses are 95% CIs. Reference categories are as follows: for size, 10–19 mm; for nonrim arterial phase hyperenhancement (APHE), absent; for enhancing capsule, absent; for nonperipheral washout, absent.

* References 29, 32, 37, 43, 44, 54, 55, 57, and 59.

† References 29, 30, 32, 33, 35–37, 40, 41, 47, 48, 53, 54, 56, 57, 60.

‡ References 29, 30, 32, 33, 35–37, 40, 41, 43, 44, 47, 48, 53–57, 59, and 60.

§ MRI and CT were compared for all major features and were only found to differ for size. The bottom rows list odds ratios for size cutoffs comparing MRI and CT, with CT as the reference standard.

Table 4: Contrast-enhanced US Multivariable Analysis

Major Feature	Odds Ratio (n = 853)*	P Value
APHE		
Not rim, not peripheral discontinuous globular	7.3 (4.6, 11.5)	.01
Rim or peripheral discontinuous globular	0.3 (0.1, 0.9)	.02
Nonperipheral washout		
Late and mild washout	4.1 (2.6, 6.6)	.01
Early (<60 sec) washout	0.3 (0.1, 0.5)	.03
Marked washout	0.7 (0.2, 2.8)	.10
Size		
<10 mm	1.1 (0.6, 2.1)	.23
≥20 mm	1.6 (1.04, 2.5)	.04

Note.—Reference categories are as follows: for size, 10–19 mm; for arterial phase hyperenhancement (APHE), absent; for nonperipheral washout, absent.

* References 34, 38, 42, 51, 52, and 58.

was also associated with HCC (OR, 4.1; 95% CI: 2.6, 6.6; P = .01). Early (<60 seconds) washout was associated with a non-HCC diagnosis (OR, 0.3; 95% CI: 0.1, 0.5; P = .03), whereas marked washout was not useful for differentiating between HCC and non-HCC (OR, 0.7; 95% CI: 0.2, 2.8; P = .10).

Prior studies exploring the diagnostic performance of LI-RADS major features for establishing HCC have mostly focused on the sensitivity, specificity, and predictive values of individual imaging features and the LI-RADS categories (62). Multivariable modeling that includes all LI-RADS major features to establish the relative strength of association of each feature with HCC may not have been possible in single centers or with study-level meta-analyses (32,63,64).

Observation size did not have an association with HCC when treated as a continuous variable at univariable analysis. Associations were observed for larger observations using cutoffs of 10, 15, and 20 mm. However, at multivariable analysis, size of at least 20 mm was not significantly associated with HCC compared with size of 10–19 mm. Size of at least 20 mm was associated with HCC for the smaller cohort with threshold growth reported, likely due to decreased interstudy variability for these observations. Interstudy variability likely also explains the difference between cohorts when comparing CT and MRI.

Our findings suggest that threshold growth is not a significant predictor of HCC relative to the other LI-RADS major features. Of note, CT/MRI LI-RADS version 2014, 2017, and 2018 were included. The criteria for threshold growth in LI-RADS version 2018 was limited to a size increase of at least 50% of a mass in no more than 6 months, whereas for LI-RADS versions 2014 and 2017, threshold growth also included a size increase of at least 100% on imaging examinations more than 6 months apart and new observations of 10 mm or larger in 24 months or less. The impact of this change could not be further explored, as the specific criterion for threshold growth using LI-RADS versions 2014 and 2017 could not be retrospectively identified.

Prior CEUS LI-RADS studies mostly explore the performance of the LI-RADS categories for HCC diagnosis (26,65–67). Our finding that both nonrim and nonperipheral discontinuous globular APHE and late and mild washout each had strong association with HCC corroborate prior works on the CEUS imaging characteristics of HCC and support the application of these as major features in the LI-RADS framework (68).

Most studies (25 of 32) had a high risk of bias. A prolonged interval between the index test and the reference standard was frequent. However, an optimal interval remains uncertain. Verification bias from tissue sampling of only a subset of observations is another frequent potential source of bias, as many lower-risk observations are less likely to have histopathologic proof. Despite the high risk of bias, a sensitivity analysis including only low-risk-of-bias studies confirmed the findings, increasing confidence in the results for the larger cohort.

Our study had several limitations. First, less than half of the eligible data sets were made available, which precluded a more detailed analysis. The findings of this study must be interpreted in the broader context of the liver imaging literature, and we recommend clinicians refer to the current version of LI-RADS until a future iteration is released. Second, threshold growth was not reported for most observations, and it remains unclear if its predictive value may differ when applied at centers that routinely perform CT/MRI within 6-month intervals. Third, ancillary features were not included, because they were incompletely reported in most studies. Fourth, comparison of extracellular and hepatobiliary contrast agents was not performed, because only one study included direct comparison of each contrast agent using the same observations, and our data set was skewed toward extracellular agent. Finally, we required only 12 months of stability to establish benignity. A longer interval might have been more specific but at the expense of sensitivity.

In conclusion, the CT/MRI and contrast-enhanced US (CEUS) Liver Imaging Reporting and Data System (LI-RADS) major features have different independent associations with hepatocellular carcinoma (HCC). Arterial phase hyperenhancement and washout pattern have strong independent associations with HCC using CT/MRI and CEUS LI-RADS. Threshold growth was infrequently reported and was not a significant independent predictor of HCC. The utility of ancillary features, which were not included in our study, would benefit from more comprehensive reporting in future research.

Acknowledgement: The authors would like to thank Alexandra (Sascha) Davis for assisting with the search strategy.

Author contributions: Guarantors of integrity of entire study, C.B.v.d.P., M.D.F.M., H.J.K., K.A.M., J.W., W.W.; study concepts/study design or data acquisition or data analysis/interpretation, all authors; manuscript drafting or manuscript revision for important intellectual content, all authors; approval of final version of submitted manuscript, all authors; agrees to ensure any questions related to the work are appropriately resolved, all authors; literature research, C.B.v.d.P., M.D.F.M., J.P.S., J.Y.C., A.F., Z.K., J.H.K., Y.Y.K., S.C.L., A.T., E.T., J.W., W.W., T.Y.; clinical studies, C.B.v.d.P., V.C., M.R.B., B.C.A., L.M.B.B., S.H.C., A.F., T.J.F., A.G., H.J., I.J., Z.K., H.J.K., J.H.K., M.J.K., S.Y.K., Y.Y.K., H.K., J.M.L., S.C.L., M.S.P., J.P., C.S.R., M.R., G.R., A.T., J.W., W.W., S.R.W., T.Y.; statistical analysis, C.B.v.d.P., M.D.F.M., J.P.S., B.L., Z.K., T.Y.; and manuscript editing, C.B.v.d.P., M.D.F.M., J.P.S., B.L., V.C., C.B.S., M.R.B., B.C.A.,

L.M.B.B., S.H.C., A.F., T.J.F., H.J., Z.K., A.S.K., G.K., S.Y.K., Y.Y.K., J.M.L., S.C.L., K.A.M., F.P., M.R., B.S., J.S.S., A.T., J.W., W.W., T.Y.

Disclosures of conflicts of interest: **C.B.v.d.P.** Disclosed no relevant relationships. **M.D.F.M.** Disclosed no relevant relationships. **J.P.S.** Disclosed no relevant relationships. **B.L.** Disclosed no relevant relationships. **V.C.** Consulting fees from Bayer, Bayer advisory board, chair of the LI-RADS Steering Committee. **C.B.S.** Grants from GE, Siemens, Philips, Bayer, Foundation of NIH, Gilead, and Pfizer (grant is to UW-Madison; UCSD is a subcontract to UW-Madison), Enanta, Gilead, ICON, Intercept, Nusirt, Shire, Synageva, Takeda; royalties from Wolters Kluwer for educational material outside the submitted work; consultation fees from Blade, Boehringer, and Epigenomics; consultation under the auspices of the University to AMRA, BMS, Exact Sciences, GE Digital, IBM-Watson, and Pfizer; honoraria to the institution from Medscape for educational material outside the submitted work; stock options in Livivos; Quantix Bio advisory board. **M.R.B.** Grants from Carmot Therapeutics, Corcept Therapeutics, CymaBay Therapeutics, Diabetes and Endocrinology Consultants, NGM Biopharmaceuticals, Madrigal Pharmaceuticals, Metacrine, Pinnacle Clinical Research, Polarean, ProSciento, and Siemens Healthineers; grants from Correct Therapeutics, ICON, and MedPace. **B.C.A.** disclosed no relevant relationships. **L.M.B.B.** Seminars for Roentgenology; expert testimony for Fadell, Cheney, and Burt. **J.Y.C.** Disclosed no relevant relationships. **S.H.C.** Research funding from and on the advisory board of Bayer Korea. **A.F.** Consulting fees from Bayer, AstraZeneca, Roche, Exact Science, and Guerbert; lecture fees from Bayer, Boston, Gilead, and Merck. **T.J.F.** Disclosed no relevant relationships. **A.G.** Disclosed no relevant relationships. **H.J.** Disclosed no relevant relationships. **I.J.** Disclosed no relevant relationships. **Z.K.** Disclosed no relevant relationships. **A.S.K.** Disclosed no relevant relationships. **H.J.K.** Disclosed no relevant relationships. **G.K.** Disclosed no relevant relationships. **J.H.K.** Disclosed no relevant relationships. **M.J.K.** Disclosed no relevant relationships. **S.Y.K.** Disclosed no relevant relationships. **Y.Y.K.** Disclosed no relevant relationships. **H.K.** Disclosed no relevant relationships. **J.M.L.** Grants from Bayer, GE Healthcare, Gerbett, Bracco, Central Medical Service, Stardmed, RF Medical, Canon Korea, Samsung Medison, Dongkug Pharma, and Vuno; lectures for Bayer, GE Healthcare, Samsung Medison, Starmed, and RF Medical. **S.C.L.** Disclosed no relevant relationships. **K.A.M.** Disclosed no relevant relationships. **L.M.** Disclosed no relevant relationships. **M.S.P.** Disclosed no relevant relationships. **F.P.** Departmental contracts with ESAOTE for cooperative research purposes and with Bracco for consultancy; honoraria from GE and Bracco for serving as a consultant; honoraria from Astrazeneca, Bayer, EISAI, IPSEN, MSD, BMS, and Samsung for lectures or presentations; honoraria from Astrazeneca, Roche, Alkermes, Tiziana Life Sciences EISAI, IPSEN, and MSD for attending advisory boards; member of the governing board of the International Contrast Ultrasound Society. **J.P.** Disclosed no relevant relationships. **C.S.R.** Disclosed no relevant relationships. **M.R.** Disclosed no relevant relationships. **G.R.** Disclosed no relevant relationships. **B.S.** Disclosed no relevant relationships. **J.S.S.** Disclosed no relevant relationships. **A.T.** Honoraria from Eli Lilly and Siemens Healthineers; former chair of the LI-RADS International Working Group. **E.T.** Disclosed no relevant relationships. **J.W.** Disclosed no relevant relationships. **W.W.** Disclosed no relevant relationships. **S.R.W.** Partial research support from Samsung for an unrelated project; equipment support from Samsung, Siemens, and Philips. **T.Y.** Consulting fees from ABC Medical Education.

References

1. American College of Radiology. Liver Reporting & Data System. https://www.acr.org/Clinical-Resources/Reporting-and-Data-Systems/LI-RADS. Published 2020. Accessed October 30, 2020.
2. van der Pol CB, Lim CS, Sirlin CB, et al. Accuracy of the Liver Imaging Reporting and Data System in Computed Tomography and Magnetic Resonance Image Analysis of Hepatocellular Carcinoma or Overall Malignancy-A Systematic Review. Gastroenterology 2019;156(4):976–986.
3. Lee S, Kim YY, Shin J, et al. CT and MRI Liver Imaging Reporting and Data System Version 2018 for Hepatocellular Carcinoma: A Systematic Review With Meta-Analysis. J Am Coll Radiol 2020;17(10):1199–1206.
4. Shin J, Lee S, Bae H, et al. Contrast-enhanced ultrasound liver imaging reporting and data system for diagnosing hepatocellular carcinoma: A meta-analysis. Liver Int 2020;40(10):2345–2352.
5. Stewart LA, Tierney JF. To IPD or not to IPD? Advantages and disadvantages of systematic reviews using individual patient data. Eval Health Prof 2002;25(1):76–97.
6. Riley RD, Lambert PC, Abo-Zaid G. Meta-analysis of individual participant data: rationale, conduct, and reporting. BMJ 2010;340:c221.
7. Riley RD, Dodd SR, Craig JV, Thompson JR, Williamson PR. Meta-analysis of diagnostic test studies using individual patient data and aggregate data. Stat Med 2008;27(29):6111–6136.
8. Cochrane. Cochrane Methods Screening and Diagnostic Tests: Handbook for DTA Reviews. https://methods.cochrane.org/sdt/handbook-dta-reviews. Published 2018.
9. McInnes MD, Bossuyt PM. Pitfalls of Systematic Reviews and Meta-Analyses in Imaging Research. Radiology 2015;277(1):13–21.
10. Frank RA, Bossuyt PM, McInnes MDF. Systematic Reviews and Meta-Analyses of Diagnostic Test Accuracy: The PRISMA-DTA Statement. Radiology 2018;289(2):313–314.
11. McGrath TA, Bossuyt PM, Cronin P, et al. Best practices for MRI systematic reviews and meta-analyses. J Magn Reson Imaging 2019;49(7):e51–e64.
12. Salameh JP, Bossuyt PM, McGrath TA, et al. Preferred reporting items for systematic review and meta-analysis of diagnostic test accuracy studies (PRISMA-DTA): explanation, elaboration, and checklist. BMJ 2020;370:m2632.
13. Cohen JF, Deeks JJ, Hooft L, et al. Preferred reporting items for journal and conference abstracts of systematic reviews and meta-analyses of diagnostic test accuracy studies (PRISMA-DTA for Abstracts): checklist, explanation, and elaboration. BMJ 2021;372(265):n265.
14. Stewart LA, Clarke M, Rovers M, et al. Preferred Reporting Items for Systematic Review and Meta-Analyses of individual participant data: the PRISMA-IPD Statement. JAMA 2015;313(16):1657–1665.
15. Kambadakone AR, Fung A, Gupta RT, et al. LI-RADS technical requirements for CT, MRI, and contrast-enhanced ultrasound. Abdom Radiol (NY) 2018;43(1):56–74. [Published correction appears in Abdom Radiol (NY) 2018;43(1):240.]
16. American College of Radiology. CT/MRI LI-RADS v2018. https://www.acr.org/Clinical-Resources/Reporting-and-Data-Systems/LI-RADS. Published 2018.
17. American College of Radiology. CT/MRI LI-RADS v2017. https://www.acr.org/Clinical-Resources/Reporting-and-Data-Systems/LI-RADS. Published 2017. Accessed May 2020.
18. American College of Radiology. CT/MRI LI-RADS v2014. https://www.acr.org/Clinical-Resources/Reporting-and-Data-Systems/LI-RADS/LI-RADS-v2014. Published 2014. Accessed November 2019.
19. American College of Radiology. CEUS LI-RADS v2017. https://www.acr.org/Clinical-Resources/Reporting-and-Data-Systems/LI-RADS. Published 2017. Accessed May 2020.
20. American College of Radiology. CEUS LI-RADS v2016. https://www.acr.org/Clinical-Resources/Reporting-and-Data-Systems/LI-RADS/CEUS-LI-RADS-v2016. https://www.acr.org/Clinical-Resources/Reporting-and-Data-Systems/LI-RADS. Published 2016. Accessed November 2019.
21. Whiting PF, Rutjes AWS, Westwood MS, et al. QUADAS-2: a revised tool for the quality assessment of diagnostic accuracy studies. Ann Intern Med 2011;155(8):529–536.
22. McInnes MDF, Moher D, Thombs BD, et al. Preferred Reporting Items for a Systematic Review and Meta-analysis of Diagnostic Test Accuracy Studies: The PRISMA-DTA Statement. JAMA 2018;319(4):388–396.
23. R Core Team. R: A language and environment for statistical computing. R Foundation for Statistical Computing, Vienna, Austria. https://www.R-project.org/. Published 2020.
24. Zhang T, Huang ZX, Wei Y, et al. Hepatocellular carcinoma: Can LI-RADS v2017 with gadoxetic-acid enhancement magnetic resonance and diffusion-weighted imaging improve diagnostic accuracy? World J Gastroenterol 2019;25(5):622–631.
25. Chen LD, Ruan SM, Lin Y, et al. Comparison between M-score and LR-M in the reporting system of contrast-enhanced ultrasound LI-RADS. Eur Radiol 2019;29(8):4249–4257.
26. Terzi E, Iavarone M, Pompili M, et al. Contrast ultrasound LI-RADS LR-5 identifies hepatocellular carcinoma in cirrhosis in a multicenter restropective study of 1,006 nodules. J Hepatol 2018;68(3):485–492.
27. Khatri G, Pedrosa I, Ananthakrishnan L, et al. Abbreviated-protocol screening MRI vs. complete-protocol diagnostic MRI for detection of hepatocellular carcinoma in patients with cirrhosis: An equivalence study using LI-RADS v2018. J Magn Reson Imaging 2020;51(2):415–425.
28. Shao S, Shan Q, Zheng N, Wang B, Wang J. Role of Intravoxel Incoherent Motion in Discriminating Hepatitis B Virus-Related Intrahepatic Mass-Forming Cholangiocarcinoma from Hepatocellular Carcinoma Based on Liver Imaging Reporting and Data System v2018. Cancer Biother Radiopharm 2019;34(8):511–518.
29. Alhasan A, Cerny M, Olivié D, et al. LI-RADS for CT diagnosis of hepatocellular carcinoma: performance of major and ancillary features. Abdom Radiol (NY) 2019;44(2):517–528.
30. Allen BC, Ho LM, Jaffe TA, Miller CM, Mazurowski MA, Bashir MR. Comparison of Visualization Rates of LI-RADS Version 2014 Major Features With IV Gadobenate Dimeglumine or Gadoxetate Disodium

in Patients at Risk for Hepatocellular Carcinoma. AJR Am J Roentgenol 2018;210(6):1266–1272.
31. An C, Park S, Chung YE, et al. Curative Resection of Single Primary Hepatic Malignancy: Liver Imaging Reporting and Data System Category LR-M Portends a Worse Prognosis. AJR Am J Roentgenol 2017;209(3):576–583.
32. Cerny M, Bergeron C, Billiard JS, et al. LI-RADS for MR Imaging Diagnosis of Hepatocellular Carcinoma: Performance of Major and Ancillary Features. Radiology 2018;288(1):118–128.
33. Chen J, Zhou J, Kuang S, et al. Liver Imaging Reporting and Data System Category 5: MRI Predictors of Microvascular Invasion and Recurrence After Hepatectomy for Hepatocellular Carcinoma. AJR Am J Roentgenol 2019;213(4):821–830.
34. Chen LD, Ruan SM, Liang JY, et al. Differentiation of intrahepatic cholangiocarcinoma from hepatocellular carcinoma in high-risk patients: A predictive model using contrast-enhanced ultrasound. World J Gastroenterol 2018;24(33):3786–3798.
35. Choi SH, Kim DH, Byun JH, et al. Subtraction Arterial Images of Hepatocyte-specific Contrast-enhanced MRI: Added Value for the Diagnosis of Hepatocellular Carcinoma in the LI-RADS v2018. The International Liver Congress. Vienna, Austria: EASL: European Association for the Study of the Liver, 2019.
36. Forner A, Darnell A, Caparroz C, et al. Evaluation of LI-RADS v2018 by Magnetic Resonance in US-detected Nodules ≤ 2 cm in Cirrhotics. The International Liver Congress. Vienna, Austria: J Hepatol 2019;70(Suppl):e73.
37. Fraum TJ, Tsai R, Rohe E, et al. Differentiation of Hepatocellular Carcinoma from Other Hepatic Malignancies in Patients at Risk: Diagnostic Performance of the Liver Imaging Reporting and Data System Version 2014. Radiology 2018;286(1):158–172.
38. Hu J, Bhayana D, Burak KW, Wilson SR. Resolution of indeterminate MRI with CEUS in patients at high risk for hepatocellular carcinoma. Abdom Radiol (NY) 2020;45(1):123–133.
39. Jeon SK, Joo I, Lee DH, et al. Combined hepatocellular cholangiocarcinoma: LI-RADS v2017 categorisation for differential diagnosis and prognostication on gadoxetic acid-enhanced MR imaging. Eur Radiol 2019;29(1):373–382.
40. Jiang H, Liu X, Chen J, et al. Man or machine? Prospective comparison of the version 2018 EASL, LI-RADS criteria and a radiomics model to diagnose hepatocellular carcinoma. Cancer Imaging 2019;19(1):84.
41. Joo I, Lee JM, Lee DH, Ahn SJ, Lee ES, Han JK. Liver imaging reporting and data system v2014 categorization of hepatocellular carcinoma on gadoxetic acid-enhanced MRI: Comparison with multiphasic multidetector computed tomography. J Magn Reson Imaging 2017;45(3):731–740.
42. Kang HJ, Kim JH, Joo I, Han JK. Additional value of contrast-enhanced ultrasound (CEUS) on arterial phase non-hyperenhancement observations (≥ 2 cm) of CT/MRI for high-risk patients: focusing on the CT/MRI LI-RADS categories LR-3 and LR-4. Abdom Radiol (NY) 2020;45(1):55–63.
43. Kang Z, Wang N, Xu A, Wang L. Digital subtract angiography and lipiodol deposits following embolization in cirrhotic nodules of LIRADS category ≥3. Eur J Radiol Open 2019;6:106–112.
44. Kierans AS, Makkar J, Guniganti P, et al. Validation of Liver Imaging Reporting and Data System 2017 (LI-RADS) Criteria for Imaging Diagnosis of Hepatocellular Carcinoma. J Magn Reson Imaging 2019;49(7):e205–e215.
45. Kim DH, Choi SH, Kim SY, Kim MJ, Lee SS, Byun JH. Gadoxetic Acid-enhanced MRI of Hepatocellular Carcinoma: Value of Washout in Transitional and Hepatobiliary Phases. Radiology 2019;291(3):651–657.
46. Kim YY, An C, Kim S, Kim MJ. Diagnostic accuracy of prospective application of the Liver Imaging Reporting and Data System (LI-RADS) in gadoxetate-enhanced MRI. Eur Radiol 2018;28(5):2038–2046.
47. Kim YY, Kim MJ, Kim EH, Roh YH, An C. Hepatocellular Carcinoma versus Other Hepatic Malignancy in Cirrhosis: Performance of LI-RADS Version 2018. Radiology 2019;291(1):72–80.
48. Lee HS, Kim MJ, An C. How to utilize LR-M features of the LI-RADS to improve the diagnosis of combined hepatocellular-cholangiocarcinoma on gadoxetate-enhanced MRI? Eur Radiol 2019;29(5):2408–2416.
49. Lewis S, Peti S, Hectors SJ, et al. Volumetric quantitative histogram analysis using diffusion-weighted magnetic resonance imaging to differentiate HCC from other primary liver cancers. Abdom Radiol (NY) 2019;44(3):912–922.
50. Lim K, Kwon H, Cho J. Inter-reader agreement and imaging-pathology correlation of the LI-RADS M on gadoxetic acid-enhanced magnetic resonance imaging: efforts to improve diagnostic performance. Abdom Radiol (NY) 2020;45(8):2430–2439.
51. Makoyeva A, Kim TK, Jang HJ, Medellin A, Wilson SR. Use of CEUS LI-RADS for the Accurate Diagnosis of Nodules in Patients at Risk for Hepatocellular Carcinoma: A Validation Study. Radiol Imaging Cancer 2020;2(2):e190014.
52. Mulazzani L, Sansone S, Giordano L, et al. Clinical validation of the role of contrast-enhanced ultrasound in the EASL guidelines for the diagnosis of hepatocellular carcinoma. The International Liver Congress. Vienna, Austria: EASL: European Association for the Study of the Liver, 2019.
53. Ronot M, Fouque O, Esvan M, Lebigot J, Aubé C, Vilgrain V. Comparison of the accuracy of AASLD and LI-RADS criteria for the non-invasive diagnosis of HCC smaller than 3 cm. J Hepatol 2018;68(4):715–723.
54. Rosiak G, Podgorska J, Rosiak E, Cieszanowski A. Comparison of LI-RADS v.2017 and ESGAR Guidelines Imaging Criteria in HCC Diagnosis Using MRI with Hepatobiliary Contrast Agents. BioMed Res Int 2018;2018:7465126.
55. Seo N, Kim MS, Park MS, et al. Optimal criteria for hepatocellular carcinoma diagnosis using CT in patients undergoing liver transplantation. Eur Radiol 2019;29(2):1022–1031.
56. Song JS, Choi EJ, Hwang SB, Hwang HP, Choi H. LI-RADS v2014 categorization of hepatocellular carcinoma: Intraindividual comparison between gadopentetate dimeglumine-enhanced MRI and gadoxetic acid-enhanced MRI. Eur Radiol 2019;29(1):401–410.
57. Stocker D, Becker AS, Barth BK, et al. Does quantitative assessment of arterial phase hyperenhancement and washout improve LI-RADS v2018-based classification of liver lesions? Eur Radiol 2020;30(5):2922–2933.
58. Terzi E, De Bonis L, Leoni S, et al. CEUS LI-RADS are effective in predicting the risk hepatocellular carcinoma of liver nodules. The International Liver Congress. Amsterdam, the Netherlands: EASL: European Association for the Study of the Liver, 2017.
59. van der Pol CB, Dhindsa K, Shergill R, et al. MRI LI-RADS Version 2018: Impact of and Reduction in Ancillary Features. AJR Am J Roentgenol 2021;216(4):935–942.
60. Zhang L, Kuang S, Chen J, et al. The Role of Preoperative Dynamic Contrast-enhanced 3.0-T MR Imaging in Predicting Early Recurrence in Patients With Early-Stage Hepatocellular Carcinomas After Curative Resection. Front Oncol 2019;9:1336.
61. Kim JH. Multicollinearity and misleading statistical results. Korean J Anesthesiol 2019;72(6):558–569.
62. Tang A, Bashir MR, Corwin MT, et al. Evidence Supporting LI-RADS Major Features for CT- and MR Imaging-based Diagnosis of Hepatocellular Carcinoma: A Systematic Review. Radiology 2018;286(1):29–48.
63. Marrero JA, Hussain HK, Nghiem HV, Umar R, Fontana RJ, Lok AS. Improving the prediction of hepatocellular carcinoma in cirrhotic patients with an arterially-enhancing liver mass. Liver Transpl 2005;11(3):281–289.
64. Rimola J, Forner A, Tremosini S, et al. Non-invasive diagnosis of hepatocellular carcinoma ≤ 2 cm in cirrhosis. Diagnostic accuracy assessing fat, capsule and signal intensity at dynamic MRI. J Hepatol 2012;56(6):1317–1323.
65. Li J, Yang L, Ma L, Lu Q, Luo Y. Diagnostic Accuracy of Contrast-Enhanced Ultrasound Liver Imaging Reporting and Data System (CEUS LI-RADS) for Differentiating Between Hepatocellular Carcinoma and Other Hepatic Malignancies in High-Risk Patients: A Meta-Analysis. Ultraschall Med 2021;42(2):187–193.
66. Huang JY, Li JW, Lu Q, et al. Diagnostic Accuracy of CEUS LI-RADS for the Characterization of Liver Nodules 20 mm or Smaller in Patients at Risk for Hepatocellular Carcinoma. Radiology 2020;294(2):329–339.
67. Ling W, Wang M, Ma X, et al. The preliminary application of liver imaging reporting and data system (LI-RADS) with contrast-enhanced ultrasound (CEUS) on small hepatic nodules (≤2cm). J Cancer 2018;9(16):2946–2952.
68. Strobel D, Seitz K, Blank W, et al. Tumor-specific vascularization pattern of liver metastasis, hepatocellular carcinoma, hemangioma and focal nodular hyperplasia in the differential diagnosis of 1,349 liver lesions in contrast-enhanced ultrasound (CEUS). Ultraschall Med 2009;30(4):376–382.